

# Axial and torsional stability of an improved single-plane and a new bi-plane osteotomy technique for supracondylar femur osteotomies

J.-M. Brinkman · C. Hurschler · A. E. Staubli ·  
R. J. van Heerwaarden

Received: 16 February 2010 / Accepted: 25 November 2010 / Published online: 15 December 2010  
© Springer-Verlag 2010

## Abstract

**Purpose** An important disadvantage of the standard medial closing-wedge distal femur osteotomy for lateral compartment osteoarthritis of the knee is the immediate effects on the extensor mechanism function. Therefore, a novel bi-plane osteotomy technique was developed. The stability and stiffness of this newly developed technique and a modification of the proximal screw configuration were tested in a composite femur model and compared to the standard single-plane technique. Research question was if the new bi-plane technique and/or modified screw configuration would improve the stability and stiffness of the construct.

**Methods** In 12 femurs, motion at the osteotomy under axial and torsion loading was measured using a 3D motion analysis system. All were subsequently tested to failure. The data recorded were used to calculate stability and stiffness of the constructs.

**Results** The stability and stiffness were highest in the bi-plane technique under axial loads, but were lower under torsional loading, compared to the single-plane technique. The screw configuration modification improved axial

stability and stiffness, but had no influence on torsional stability.

**Conclusion** In replicate femurs, the new bi-plane technique improved axial stability, but in contrast to what was theorized, decreased torsional stability, compared to the single-plane technique. The addition of a bi-cortical screw proximally improved stability under axial loading, but not torsion. Further clinical testing will have to prove if early full weight bearing using the new bi-plane technique is possible.

**Keywords** Distal femur · Primary stability · Osteotomy technique

## Introduction

Distal femoral supracondylar osteotomies (SCO) can be performed using either lateral opening or medial closing-wedge techniques [4, 5, 16]. Biomechanically, the medial closing-wedge technique offers superior initial stability and stiffness [4]. An important disadvantage of the standard single-plane medial closing-wedge technique is the position of the osteotomy relative to the trochlea and the soft tissues gliding surface on the anterior side of the femur. The saw cuts of the osteotomy need to be positioned proximal to the trochlea avoiding the patella-femoral joint. The osteotomy does disrupt the soft tissue gliding mechanism however causing a haematoma, and subsequent pain and swelling, slowing rehabilitation. Therefore, a modification of the oblique medial closing-wedge technique was developed by one of the authors (AES): the bi-plane medial closing-wedge technique [7, 11].

At our institution, we previously tested the primary stability and stiffness of different SCO configurations using

---

J.-M. Brinkman (✉) · R. J. van Heerwaarden  
Department of Orthopaedics, Limb Deformity Reconstruction  
Unit, Sint Maartenskliniek, P.O. Box 8000,  
3440 JD Woerden, The Netherlands  
e-mail: justusmartijn@gmail.com

C. Hurschler  
Laboratory for Biomechanics and Biomaterials,  
Orthopaedic Department, Hannover Medical School,  
Anna-von-Borries-Strasse 1-7, 30625 Hannover, Germany

A. E. Staubli  
Department of Orthopaedic Surgery, Privatklinik Sonnmatt,  
Hemschenstrasse, 6000 Lucerne 15, Switzerland

axial and torsional cyclical loading, in a composite biomechanical femur model, avoiding the availability problems and inter-specimen variability associated with cadaver specimens [4]. The structural equivalence of these composite femurs with human bones has been validated [13, 19].

Compared to the single-plane technique, in the bi-plane technique, the two saw cuts for the closing wedge are made only in the posterior 3/4 of the femur after which an ascending oblique saw cut is performed on the anterior surface of the femur, completing the osteotomy (Fig. 1). The ascending saw cut enables a more distal positioning of the closing-wedge saw cuts; the soft tissue gliding mechanism is not disrupted as the anterior ascending bone cut ends more proximal on the anterior cortex, avoiding the patella-femoral compartment (Fig. 1). Furthermore, the ascending saw cut increases the corticospongious contact area, which should in theory further enhance stability, especially under torsion loads, and promote bone healing. A bi-cortical proximal screw was added, instead of the four uni-cortical screws used previously, as a potential way to further enhance the stability of the construct (Fig. 1). The use of the extra bi-cortical screw was adopted from high tibial osteotomies (HTO) fixated with Tomofix, in which the authors use one bi-cortical and 3 uni-cortical screws distal to the osteotomy [2].

The purpose of this study is to test these two modifications of the standard SCO technique with angle stable medial distal femur plate (MDF) fixation. In the current study, using the same femur model, loading protocols and measuring technique [4], we set out to test: (1) the stability and stiffness of the newly developed bi-plane technique, (2) the influence on stability and stiffness of the modified screw configuration and (3) compare results to those from the previous biomechanical study.

## Materials and methods

The same test set-up and loading protocols as described in detail in a previous similar biomechanical SCO study were used [4]. In the present study, twelve short-glass-fibre-reinforced (SGFR) third-generation composite replicate femurs (Sawbones Europe AB, Malmö, Sweden) were used in two configurations: (1) MDF SP: single-plane oblique medial closing-wedge SCO fixated with a medial angle stable implant (Tomofix, Synthes, Bettlach, Swiss) and (2) MDF BP: bi-plane oblique medial closing-wedge SCO (Fig. 1). Six femurs were available for each configuration, all femurs were subjected to axial and torsion loads and all were subsequently tested to failure (Table 1).

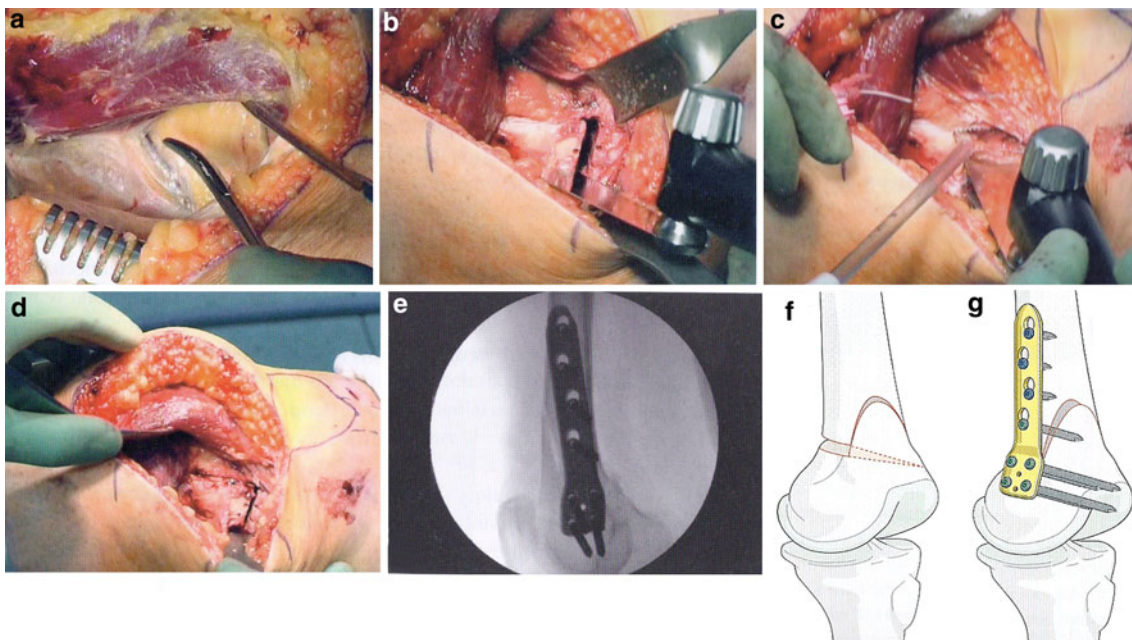


**Fig. 1** a–e Intra-operative view, a soft tissues on the anterior side of the femur, b standard wedge has been removed in posterior three-fourth, thin saw blade is introduced for ascending saw cut, c anterior saw cut, d osteotomy has been closed; the soft tissues are still intact, e per-operative lateral image intensifier view of the osteotomy. f and

g schematic view of the bi-plane osteotomy, f before closure, g with the MDF plate in place, note the bi-cortical proximal screw (Figure 1 is reprinted from [11], with permission of AO publishing, Dübendorf, Swiss)

**Table 1** Overview of the configurations and test protocol

Total	OT type	No	No runs Axial loading	No cycles	Axial preload (N)	Loading	Torsional preload (Nm)	Loading
Axial								
12	MDF SP	6	1	100	10	150 N	–	–
	MDF BP	6	2	100	10	800 N	–	–
			3	1	–	To failure	–	–
Total	OT type	No	No runs Torsional loading	No cycles	Axial preload (N)	Loading	Torsional preload (Nm)	Loading
Torsion								
12	MDF SP	6	1	100	–	–	0.5	5 Nm
	MDF BP	6	2	100	150	–	0.5	5 Nm
			3	100	800	–	0.5	5 Nm
			4	1	–	–	–	To failure

An overview of the number of femurs, test runs in axial and torsional loading, number of cycles and loading protocols that were used to test the two osteotomy (OT) types (MDF SP single-plane, MDF BP bi-plane) is shown

### Experimental set-up

The osteotomies were performed and plates implanted according to the standard surgical procedure for each implant as provided by the manufacturer [11]. Distally, 4 bi-cortical screws were used for fixation. Proximally, 3 uni-cortical screws and 1 bi-cortical screw were used. A wedge of 10 degrees ( $^{\circ}$ ) was removed with the distal saw cut directed  $20^{\circ}$  oblique to the distal femur condylar line.

All composite femurs were aligned in a standardized way using an alignment jig and a femur saw guide (Balansys<sup>®</sup>, Mathys Medical, Bettlach, Swiss), which provided a reproducible osteotomy position, osteotomy direction and wedge size. The bone deformation needed for the closing of the wedge and the implant fixation was possible without producing a fracture in the lateral bone bridge. The femur head and trochanter and the distal femur end were thereafter embedded in a polyurethane-based cold-curing resin (Ureol FC 53, Vantico GmbH, Wehr, Germany) in a specially constructed fixture; the fixture allowed for mounting of the femur in a materials testing machine (MTS Mini Bionix, MTS Systems Corporation, Eden Prairie, MN, USA). The fixture was designed in such a way that a mechanical femur loading axis of  $2^{\circ}$  was created [14, 15].

### Measuring system

The principles of rigid body motion were used to measure (micro) motion across the SCO. Reference point pairs, relative to which motion was measured, were defined on the replicate femur; two points across the midpoint of the intact lateral cortical bridge, two points midway across the osteotomy and two points just posterior of the plate on

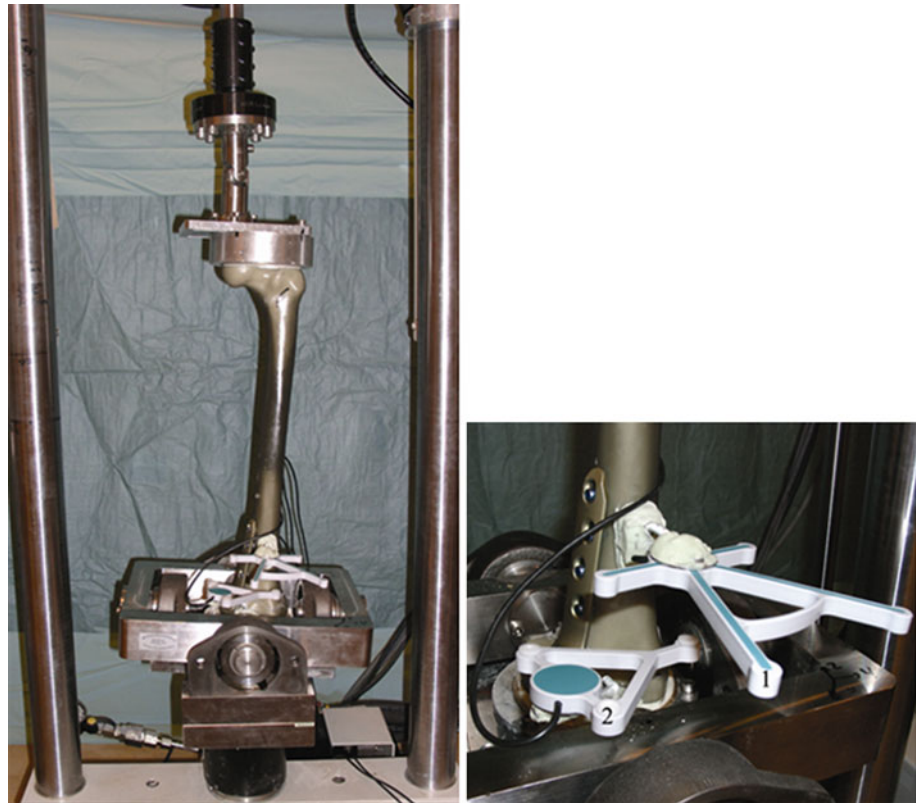
the medial side of the femur; a digital ruler was used to reproducibly determine the position of the point pairs. Motion across the osteotomy was measured using the same ultrasound 3D motion analysis system as in our previous biomechanical study (CMS20S, Zebris Medizintechnik, GmbH, Isny, Germany) [4]. The accuracy of the system as reported by the manufacturer is 0.01 mm (Zebris Medizintechnik, GmbH, Isny, Germany). The sensor and emitter markers were rigidly fixed to the femur using bone cement (Palacos, Biomet, Inc, Warsaw, Indiana, USA), at the same position on each femur (Fig. 2). After mounting of the femur in the MTS with the microphone template attached, a coordinate system was defined based on landmarks on the distal femur using a calibrated pointer device.

### Loading protocol

The replicate femurs were subjected to axial and torsional loading protocols designed to simulate physiological loading, with all femurs subjected to axial loading and torsional loading (Table 1). After an axial preload of 10 N was achieved, the femurs were tested during 100 cycles for each load (150 N and 800 N) at a rate of 0.5 Hz. Six femurs (3 for each configuration) were subsequently tested to axial failure under displacement control at a rate of 0.1 mm per second. Failure was defined by a drop of actuator loading, because of failure of the bone, bone-implant construct or of the implant itself.

Each femur was subjected to 100 cycles of 5Nm torque at a rate of 0.25 Hz; the first run was done without an axial preload; thereafter, two runs using 150 and 800 N axial preloads, respectively, were performed. After completion of all three runs, six femurs (3 per configuration) were tested to torsional failure under displacement control at a

**Fig. 2** *Left* Test set-up: The replicate femur is loaded in the MTS. *Right* Close-up of the measuring system; microphone (1) and speaker (2) templates are rigidly fixed to the replicate femur close to the osteotomy



rate of  $0.25^\circ$  per second. Criteria for failure were the same as used for the axial loading failure tests.

#### Statistical analysis

The displacement data recorded using the 3D measuring system were computed using a custom-made program in Mathematica (Version 5.0, Wolfram research, Inc, Champaign, IL, USA). Displacement at the SCO was calculated using the change in the (absolute) distance between the measuring points per loading cycle. The amount of motion that occurs at the SCO was defined as the difference between the maximum increase and maximum decrease in the distance between measuring points determined for each cycle and per measuring point. A greater mean difference calculated over 100 cycles and three measuring points indicates more motion allowed by the bone–implant construct. Stability was defined as the amount of motion allowed by the construct in the axial and torsion tests.

The axial stiffness of the construct was calculated by plotting displacement at the SCO during the failure test, defined as the average amount of movement on the Z-axis of the three previously defined point pairs, against the force data. Stiffness of the bone–implant construct was defined as the slope of the linear portion of the force–osteotomy deformation curve (i.e., the force required per mm of displacement). Similarly, stiffness in torsion was calculated

by plotting the rotation around the Z-axis over time against the moment (Nm) applied by the MTS and defined as Nm required for one degree of rotation.

Results of both techniques were compared to the motion data from our previous biomechanical SCO study; the data from the single-plane oblique medial closing-wedge SCO fixated with the same angle stable implant (MDF) using the old screw configuration were used for comparison [4].

Statistical analysis was performed using SPSS statistical software (Version 17, SPSS, Inc., Chicago, IL, USA); the independent samples *T* test was used to measure statistical differences between configurations, and *P* values  $<0.05$  were considered significant using a 95% confidence interval ( $CI_{95}$ ). The data collected in this study were not statistically compared to that from the previous study because the measurements were performed at different study periods.

#### Results

Axial and torsion test results are displayed in the tables and figures; for comparison purposes, the results from the single-plane, medial closing-wedge OT, with 4 uni-cortical screws proximally (MDF) from the previous SCO study, are also displayed.



**Table 2** Axial and torsion test results

OT type	Axial load (N)	Torsion load (Nm)	Axial preload (N)	N cycles	Mean $\pm$ SD	95% CI for mean		Min	Max	SE
						Lower bound	Upper bound			
MDF SP	150			600	0.054 $\pm$ 0.025	0.052	0.056	0.02	0.19	0.001
MDF BP	150			600	0.044 $\pm$ 0.018	0.043	0.046	0.016	0.14	0.0007
MDF	150			300	0.07 $\pm$ 0.043	0.065	0.075	0	0.26	0.0025
MDF SP	800			600	0.061 $\pm$ 0.019	0.059	0.062	0.03	0.22	0.0008
MDF BP	800			600	0.056 $\pm$ 0.017	0.055	0.058	0.025	0.11	0.00071
MDF	800			300	0.11 $\pm$ 0.03	0.1	0.11	0.037	0.18	0.0017
MDF SP		5	0	600	0.049 $\pm$ 0.013	0.048	0.05	0.018	0.12	0.0005
MDF BP		5	0	600	0.069 $\pm$ 0.016	0.067	0.07	0.032	0.14	0.0006
MDF		5	0	300	0.053 $\pm$ 0.017	0.051	0.055	0.015	0.11	0.001
MDF SP		5	150	600	0.05 $\pm$ 0.015	0.049	0.051	0.019	0.15	0.0006
MDF BP		5	150	600	0.069 $\pm$ 0.016	0.067	0.070	0.03	0.14	0.0006
MDF		5	150	300	0.045 $\pm$ 0.018	0.043	0.047	0.0057	0.1	0.0011
MDF SP		5	800	600	0.049 $\pm$ 0.012	0.048	0.05	0.018	0.11	0.0005
MDF BP		5	800	600	0.07 $\pm$ 0.016	0.07	0.072	0.031	0.15	0.0007
MDF		5	800	300	0.044 $\pm$ 0.015	0.042	0.045	0.014	0.13	0.0009

Results for the axial and torsion tests are shown; osteotomy type, axial load, total number of cycles and the mean displacement, including the standard deviation (SD), CI<sub>95</sub> and Minimum and Maximum, are detailed

### Axial loading

No visible damage to bone, bone–implant construct or implant was found.

During each cycle of loading and unloading, a corresponding movement at the osteotomy was observed to occur. At 150 and 800 N, the MDF BP allowed less motion than the MDF SP, and the difference in motion was statistically significant ( $P < 0.005$ ) at both loading levels (Table 2; Fig. 3).

### Axial failure tests

All 6 failure tests resulted in a per-trochanteric femoral neck failure, i.e. failure occurred proximally to the osteotomy in the replicate femurs. No macroscopically observable failure at the bone–implant interface or of the implant itself was observed. No fractures of the opposing lateral cortex bone bridge were observed in both techniques. During the axial failure tests, the force time course of loading typically demonstrated increasing motion with increasing axial compression load with a sudden drop in load at failure. Calculated stiffness was highest in the MDF BP configuration, and the difference was statistically significant ( $P = 0.013$ ) (Table 3; Fig. 4).

### Torsional loading

No visible damage to bone, bone–implant construct or implant was found.

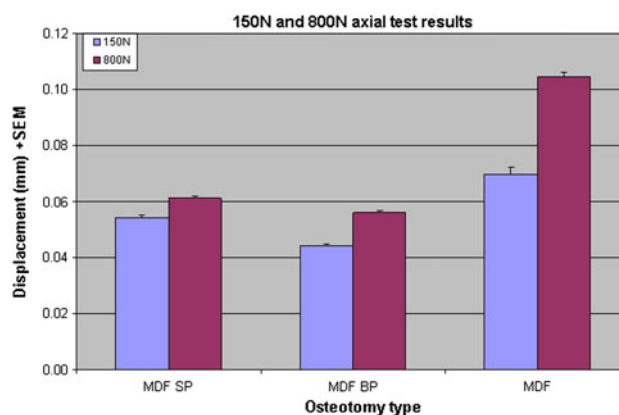


**Fig. 3** Results for both the 150 and 800 N axial compression tests; results for each test is displayed for each modality; displacement is displayed in millimetres (mm). The standard error of the mean is also shown (SEM)

In all tests, the MDF SP configuration allowed less motion; differences were statistically significant ( $P < 0.005$ ) in all tests (Table 2; Fig. 5).

### Torsional failure tests

In all six femurs, similar patterns of failure were observed, the opposing lateral cortex bone bridge fractured first, after which a fracture occurred at the screw–bone interface in all femurs. Calculated stiffness was greatest in the MDF SP configuration, the difference was not statistically significant (Table 3; Fig. 6).

**Table 3** Axial and torsion failure test results

Osteotomy type	Axial stiffness					Torsional stiffness				
	<i>N</i>	Mean	SD±	Min	Max	<i>N</i>	Mean	SD	Min	Max
MDF SP	3	7,169	3,303	4,850	10,952	3	44.4	10.4	26.4	35.8
MDF BP	3	19,363	3,746	17,164	23,690	3	31.9	4.9	33.4	54.3
MDF	3	5,723	990	4,618	6,528	3	28.4	3.2	26	32.1

Results for the axial and torsional failure tests are shown; the number of femurs (*N*), mean stiffness and minimum and maximum are detailed. Axial stiffness is in N/mm and torsional stiffness in Nm/°

**Fig. 4** Results for the axial failure tests; stiffness is displayed in Nm per millimetre displacement on the Z-axis. The SEM is also shown

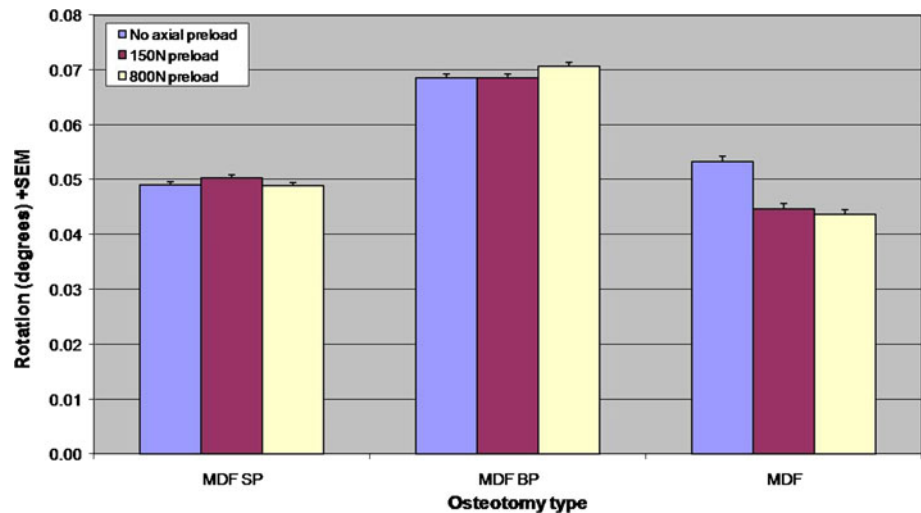
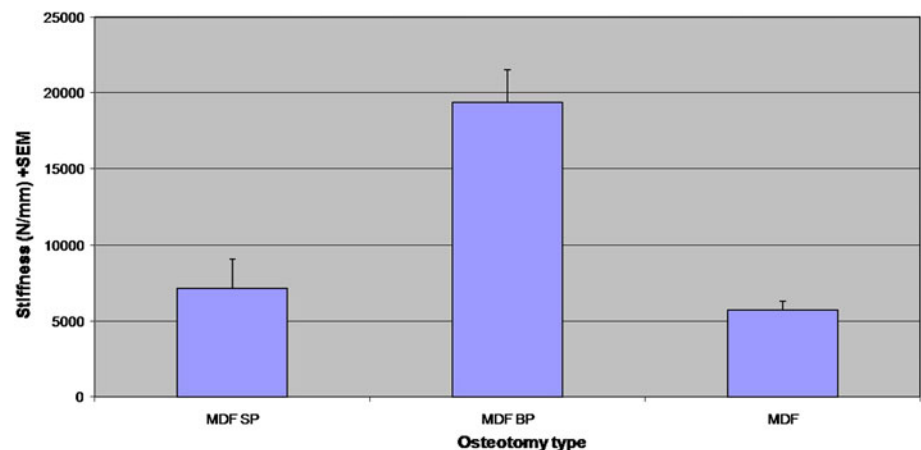


**Fig. 5** Results for the torsional test runs; results for each test are displayed for each modality; rotation is displayed in degrees rotation. The SEM is also shown



One important difference was observed: in the MDF BP, the fracture at the lateral cortex started at the point where the anterior part of the bi-plane osteotomy ends at the intact lateral cortical hinge of the femur and ran into the lateral femur condyle; concurrently, the anterior portion of the bi-plane osteotomy fractured off (Fig. 7).

## Discussion

The most important finding in the present study is that the new bi-plane technique improved axial stability, but in

contrast to what was theorized, had a decreased stability in torsion, compared to the single-plane technique.

The MDF in the previous study only differs from the MDF SP in this study in the screw configuration used proximally; four uni-cortical screws, instead of three and one bi-cortical in the current set-up [4]. Comparison shows that the MDF in the previous study is less stable under axial loading than both configurations in the current study (Fig. 3). This is in part because of the extra bi-cortical screw. However, the MDF BP has a statistically significant higher stability than the SP technique under axial loading. Thus, the bi-plane osteotomy itself also increases axial stability. Furthermore, in the axial

**Fig. 6** Results for the torsional failure tests; stiffness is displayed in Nm per degree rotation around the Z-axis. The SEM is also shown

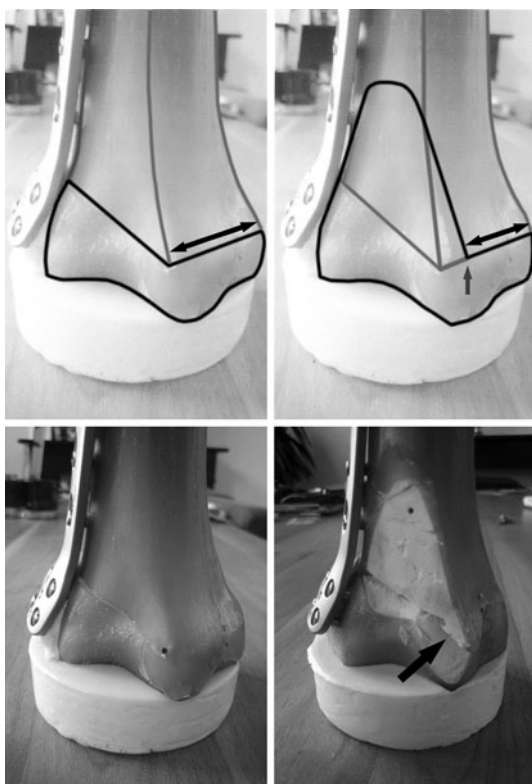
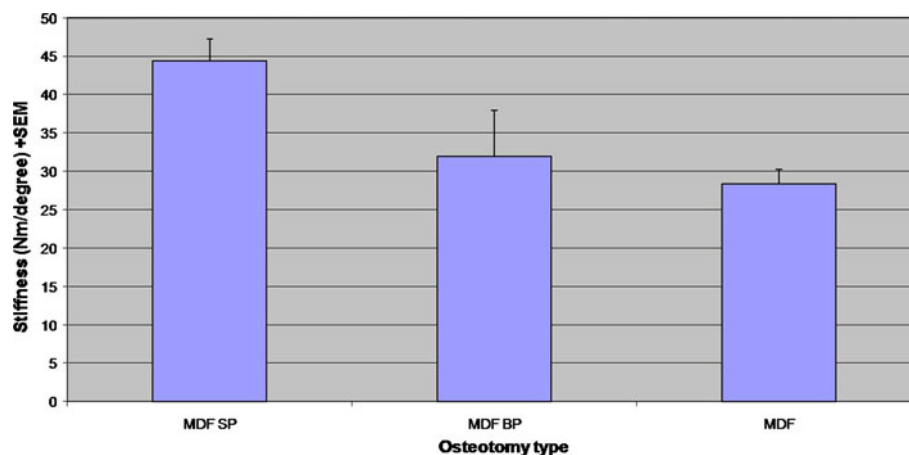


**Fig. 7** View of SP (left) and BP (right) techniques, outlined in black is the shape of the distal part of the OT. Grey arrow (top right): the ascending saw cut endpoint on the lateral cortex. Black arrows (top left and right): the size of the intact lateral cortical hinge. Clearly visible (bottom left and right) is the difference in fracture pattern of the lateral cortex in the torsion failure test. Black arrow (bottom right): the lateral cortex fracture at the endpoint of the ascending saw cut

failure tests, MDF BP has a much higher calculated stiffness than MDF SP and MDF (Fig. 5). A possible explanation is that the energy is distributed and absorbed across a larger area in the bi-plane technique.

In contrast to the axial stiffness and stability, and instead of what was theorized, the bi-plane technique showed

decreased stability in the torsion tests (Fig. 4). Possible explanations for this are that on the lateral cortex in the AP direction, forces are distributed across a smaller area (Fig. 7). The fracturing off of the anterior part of the osteotomy suggests that it does not contribute to stability. Furthermore, judging from the fracture pattern in the torsional failure tests, the point where the standard oblique and new anterior saw cut join on the lateral side of the femur is not very stable. In the MDF SP, there is no disruption of the lateral cortex because of the second saw cut, and the two flat ends of the osteotomy lie rigidly against each other, and the entire AP diameter of the lateral cortex contributes to stability (Fig. 7). The MDF and MDF SP perform similarly in the torsion tests; it therefore appears that the bi-cortical screw does not improve stability in torsion. MDF SP does have a higher calculated stiffness in the torsion to failure test; however, this might be because it has no weak hinge point and has the extra bi-cortical screw proximally. Interestingly, in contrast to its torsional stability, MDF BP has a higher calculated stiffness than MDF. The bi-cortical screw therefore appears to influence stiffness but not stability in torsion.

In biomechanical tests of high tibial osteotomies (HTO) using replicate tibia sawbones, Agneskirchner et al. found significantly improved stability using the TomoFix HTO plate [1]. Based on these results and clinical observations of patients starting full weight bearing earlier than prescribed in the rehabilitation protocol, clinical studies were performed comparing an early full weight bearing protocol to a standard weight bearing protocol after HTO [3]. Subsequently, early full weight bearing has been introduced as standard protocol after HTO [3, 20, 21]. For SCO in clinical studies reporting on the single-plane technique with the angle stable TomoFix MDF implant used in this study, no bone-healing problems have been reported with a standard rehabilitation protocol consisting of 6–8 weeks of partial weight bearing [6, 7, 10]. No bone-healing problems have been observed in the first cohort of 30 patients

operated on with the bi-plane technique either [8]. After introduction of the bi-plane technique, a faster recovery of knee function was observed when compared with the single-plane patient groups, and patients themselves increased the amount of weight bearing within the first 6 weeks after the osteotomy, although full weight bearing was allowed after 6–8 weeks only if clear signs of bone healing were visible. Repeatedly, instead of what was advised, patients were bearing full weight without crutches at the time of their first follow-up. In these patients, no corrections loss and no impaired bone healing had been found [8].

The findings regarding torsional stability in the current study are to some extent in contrast with the observation that patients experience their osteotomy as stable. The amount of motion observed in the torsion test may be the cause for concern; however, no damage to the construct was observed during the various torsion tests and in the failure tests, stiffness appeared to be less affected negatively by the bi-plane osteotomy. It might be that stability in torsion is less important than axial stability, with the decreased torsion stability still being in the range of what is required for the construct to be stable. However, no fatigue tests were performed, so no conclusions on longer-term effects of repeated torsion loading on the osteotomy can be drawn. Therefore, post-operatively, physical activities, which produce high torsional loads on the femur, such as leg movements in breaststroke swimming, are probably best avoided until bone healing has been observed.

Specific limitation of torsional motion has not been described after osteotomies around the knee. Knee braces have been used to limit rotation in knees with ligamentous laxities, i.e., preventing torsion of the tibia relative to the femur [17, 23]. The use of braces for additional stability after SCO has been documented by various authors; Healy et al. used a brace if the fixation of the osteotomy was questionable; both Wang et al. and Miniaci et al. also used braces [9, 18, 22]. All three authors in their series of patients used an angled blade plate for fixation and a limited weight bearing protocol initially, varying from non-weight bearing to toe touch for 6 weeks, full weight bearing being allowed after 12 weeks or if clear signs of consolidation were present on follow-up radiographs. Based on the results of the present study, a clinical study has been started at our institution using early full weight bearing and a hinged brace until full bone healing in patients after bi-plane SCO fixated with the angle stable implant used in this study [12].

Important limitations of the study are, as in the previous study, the limited amount of femurs available for the failure tests; exact conclusions on stiffness might not be possible. Also, because of the size of the data collected by the 3D measuring system, no fatigue tests could be performed. Furthermore, no test–retest reliability measurements were

performed. Ideally, the MDF data should have come from the same series of tests, not the previous study. Because of this, no statistical comparison to the current data was performed.

## Conclusion

In the current test configuration, the new bi-plane technique improved axial stability, but in contrast to what was theorized, decreased torsional stability, compared to the single-plane technique. The addition of a bi-cortical screw proximally improved stability under axial loading, but not torsion. Further clinical testing will have to prove if early full weight bearing using the new bi-plane technique is possible.

## References

1. Agneskirchner JD, Freiling D, Hurschler C, Lobenhoffer P (2006) Primary stability of four different implants for opening wedge high tibial osteotomy. *Knee Surg Sports Traumatol Arthrosc* 13:291–300
2. Brinkman JM, Lobenhoffer P, Agneskirchner JD, Staubli AE, Wymenga AB, van Heerwaarden RJ (2008) Osteotomies around the knee: patient selection, stability of fixation and bone healing in high tibial osteotomies. *J Bone Joint Surg Br* 90:1548–1557
3. Brinkman JM, Luites JW, Wymenga AB, van Heerwaarden RJ (2010) Early full weight bearing is safe in open-wedge high tibial osteotomy—RSA analysis of postoperative stability compared to delayed weight bearing. *Acta Orthop* 81:193–198
4. Brinkman JM, Hurschler C, Agneskirchner JD, Freiling D, van Heerwaarden RJ (2010) Axial and torsional stability of supracondylar femur osteotomies: biomechanical comparison of the stability of five different plate and osteotomy configurations. *Knee Surg Sports Traumatol Arthrosc*. doi:10.1007/s00167-010-1281-3
5. Franco V, Cipolla M, Gerullo G, Gianni E, Puddu G (2004) Open wedge osteotomy of the distal femur in the valgus knee. *Orthopaed* 33:185–192
6. Freiling D, Van Heerwaarden RJ, Lobenhoffer P (2007) Femurosteotomien: Wann muss ich an das Femur? *Orthopädische Praxis* 43:136–142
7. Freiling D, Lobenhoffer P, Staubli A, van Heerwaarden RJ (2008) Die varisierende schließende Femurosteomie zur Behandlung der Valgusarthrose am Kniegelenk. *Arthroscopie* 21:6–14
8. Freiling D, van Heerwaarden R, Staubli A, Lobenhoffer P (2010) Die varisierende closed-wedge Osteotomie am distalen Femur zur Behandlung der unikompartimentalen lateralen Arthrose am Kniegelenk. Medial closed-wedge osteotomy of the distal femur for the treatment of unicompartimental lateral osteoarthritis of the knee. *Oper Orthop Traumatol* 22:317–334
9. Healy WL, Anglen JO, Wasilewski SA, Krackow KA (1988) Distal femoral varus osteotomy. *J Bone Joint Surg Am* 70:102–109
10. van Heerwaarden RJ, Wymenga AE, Freiling D, Lobenhoffer P (2007) Distal medial closed wedge varus femur osteotomy stabilized with Tomofix plate fixator. *Oper Tech Orthop* 17:12–21
11. van Heerwaarden RJ (2008) Supracondylar varization osteotomy of the femur with plate fixation. In: Lobenhoffer P, van



- Heerwaarden RJ, Staubli AE, Jakob RP (eds) Osteotomies around the knee. Georg Thieme Verlag, Stuttgart, pp 147–166
12. van Heerwaarden RJ, Brinkman JM, Hurschler C (2010) Superior axial stability of a new biplane osteotomy technique for supracondylar femur osteotomies fixed with an angular stable plate. *Knee Surg Sports Traumatol Arthrosc* 18 (suppl 1): SCP10–1068
  13. Heiner AD, Brown TD (2001) Structural properties of a new design of composite replicate femurs and tibias. *J Biomech* 34:773–781
  14. Hsu RW, Himeno S, Coventry MB, Chao EY (1990) Normal axial alignment of the lower extremity and load-bearing distribution at the knee. *Clin Orthop Relat Res* 255:215–227
  15. Luo CF (2004) Reference axes for reconstruction of the knee. *Knee* 11:251–257
  16. Marti RK, Schroeder J, Witteveen A (2000) The closed wedge varus supracondylar osteotomy. *Oper Tech Sports Med* 8:48–55
  17. Mathewson PR, Greenwald RM (2003) Reduction in anterior cruciate ligament load and tibiofemoral rotation under applied axial rotation: a surrogate model study of the efficacy of a new knee derotation brace concept. *JPO* 15:1–8
  18. Miniaci A, Grossmann SP, Jakob RP (1990) Supracondylar femoral varus osteotomy in the treatment of valgus knee deformity. *Am J Knee Surg* 3:65–73
  19. Szivek JA, Weng M, Karpman R (1990) Variability in the torsional and bending response of a commercially available composite “femur”. *J Appl Biomater* 1:183–186
  20. Takeuchi R, Aratake M, Bito H, Saito I, Kumagai K, Ishikawa H, Akamatsu Y, Sasaki Y, Saito T (2008) Simultaneous bilateral opening-wedge high tibial osteotomy with early full weight-bearing exercise. *Knee Surg Sports Traumatol Arthrosc* 16:1030–1037
  21. Takeuchi R, Ishikawa H, Aratake M, Bito H, Saito I, Kumagai K, Akamatsu Y, Saito T (2009) Medial opening wedge high tibial osteotomy with early full weight bearing. *Arthroscopy* 25:46–53
  22. Wang JW, Hsu SS (2005) Distal femoral varus osteotomy for osteoarthritis of the knee. *J Bone Joint Surg Am* 87:127–133
  23. Wojtyś EM, Loubert PV, Samson SY, Viviano DM (1990) Use of a knee-brace for control of tibial translation and rotation. A comparison, in cadavera, of available models. *J Bone Joint Surg Am* 72:1323–1329